Adaptive Forward Identification and Auto-Tuning for Motor Velocity Control

T. Kitade†, H. Ohmori†, A. Sano†, T. Miyashita‡, H. Nishida‡, and Y. Todaka‡

†Department of System Design Engineering, Keio University,
3-14-1 Hiyoshi, Kohoku-ku, Yokohama 223-8522, Japan

‡Industrial Systems Division, Fuji Electric Corporation,
Hino, Tokyo 191-

Abstract: This paper presents a new on-line adaptive identification of physical model parameters by adjusting the parameters in the feedforward controller and feedback PI controller for a motor drive system. The proposed scheme is characterized by new set-up of a suitable reference model which generates signals needed to identify the physical parameters of a two-mass motor system, such as inertia moments of motor and load, shaft conductance, viscous friction terms proportional to motor velocity and squared velocity, and Coulomb friction. The adaptive algorithm not only can give the model parameters but also compensate for the unknown friction effects by adjusting the feedforward controller. Stability is also investigated via the ASPR property of the controlled system. The effectiveness of the proposed scheme is examined in simulation and experiment of speed control of a two-mass motor system.

1. Introduction

In motor velocity control, uncertain inertia moment and nonlinear frictions sometimes degrade its control performance [1]. Various robust control approaches have been exploited previously [2]-[4], however, fine tuning of the controller parameters is essentially needed in motor drive systems to attain high tracking performance and quick recovery response for stepwise torque disturbances [5]. The closed-loop identification using only input and output data (control torque input and motor velocity) can hardly attain the identifiability in practical situations. Instead of such a direct identification scheme, an indirect approach will be effective in the closed-loop identification of the physical model parameters.

Therefore, the aim of this paper is to present a new scheme for adaptive identification of physical model parameters by adjusting the parameters in a feedforward controller and feedback PI controller for motor velocity control. The proposed scheme is characterized by new set-up of a suitable reference model which generates signals needed to identify the physical parameters in two-mass motor system, such as inertia moments of motor and load, shaft conductance, viscous friction terms proportional to motor velocity and squared velocity, and Coulomb friction. Comparing with ordinary closed-loop identification directly using the input-output data of motor drive system, the proposed feedforward approach can have quick convergence and less effect of disturbances, since the adaptive algorithm uses only signals generated by the feedforward controller except the output tracking error. The convergence of the adaptation algorithm is also investigated via the almost strictly positive real (ASPR) property of the controlled system [6]. The effectiveness of the proposed approach is examined in numerical simulation and experiment for velocity control of two-mass induction motor with unknown inertia ratio.

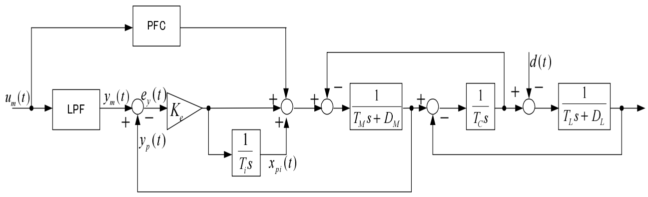

Figure 1: Two degree-of-freedom motor velocity control

2. Two-Degree-Freedom Velocity Control

Fig.1 illustrates a typical two degree-of-freedom motor velocity control system for a two-mass motor. The PI controller is employed to compensate for the closed-loop response to stepwise torque disturbances. If the behavior of the motor and load is described by an equivalent one-mass system with $1/(T_M + T_L)$ and no nonlinear frictions exist, the PI parameters K_e and T_i can be designed as follows: Since K_e corresponds to the proportional gain of the PI controller, then the closed-loop dynamics consisting of the PI controller and the equivalent system can be described by a second-order linear transfer function with the denominator as

$$s^2 + \frac{T_i D_M + K_e T_i}{T_i(T_M + T_L)} s + \frac{K_e}{T_i(T_M + T_L)} \qquad (1)$$

which is characterized by the natural frequency $\omega_n =$

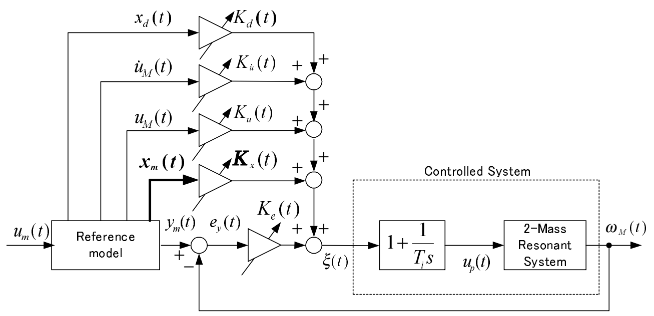

Figure 2: Schematic diagram of total control system

$\sqrt{K_e/T_i(T_M+T_L)}$ and the damping factor $\zeta = (K_e + D_M)\sqrt{T_i}/2\sqrt{K_e(T_M+T_L)}$. If the cutoff frequency ω_c of the loop transfer system is specified as $\sqrt{\phi}\cdot\omega_n$ where ϕ is chosen as 2, for instance, the PI controller parameters can be given as $K_e = \omega_c T_M$ and $T_i = \phi/\ \omega_c$. Thus, the damping factor of the closed-loop system is given by $\zeta = \sqrt{\phi}(\omega_c T_M + D_M)/(2\omega_c T_M)$, and then it becomes approximately 0.7 if $D_M = 0$ and $\phi = 2$. However, if the motor parameters T_M and D_M are uncertain, the tuning of the PI controller parameters is needed. Moreover, if the motor is subjected to unknown nonlinear frictions, adaptive compensation is also needed to compensate for the degraded performance [1].

3. Adaptive Identification of Physical Parameters

Fig.2 illustrates the proposed scheme for adaptive identification of physical model parameters and compensator tuning in a feedforward manner in velocity control of two-mass motor. The block surrounded by the broken line includes the PI controller with unity gain and the two-mass motor with nonlinear friction. The friction terms include viscous friction proportional to velocity and squared velocity, and the Coulomb friction as stated later. Conventionally these model parameters are identified by using the input/output data $\{u_p(t),\ \omega_M(t)\}$ of the controlled system. However, the convergence of the parameters is affected by disturbances, and adaptive algorithms for rejecting the influences tend to be complicated. In the proposed feedforward modeling approach, the adaptive parameters $\boldsymbol{K}_d(t)$, $K_{\dot{u}}(t)$, $K_u(t)$ and $\boldsymbol{K_x}(t)$, and the PI gain $K_e(t)$ are adjusted by forcing the output error $e_y(t)$ to zero, where the output error is defined by

$$e_y(t) = y_m(t) - \omega_M(t) \tag{2}$$

where $\omega_M(t)$ is the motor velocity and $y_m(t)$ is the reference velocity. The proposed configuration is based on the simple adaptive control(SAC) scheme [], however the ordinary SAC scheme has taken care of no converged values of the adustable parameters. On the other hand, the purpose of this paper is to give a new algorithm for adaptively providing all the physical parameters in the two-mass system from the adjustable parameters in the feedforward paths, by sophisticatedly constructing the

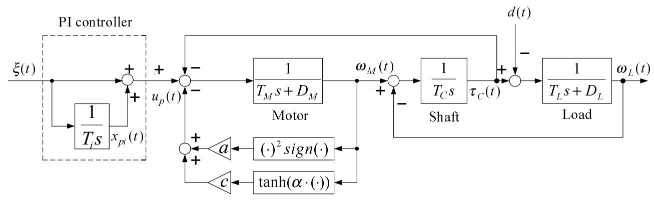

Figure 3: Controlled two-mass resonant system

reference model, as described later. The reference input $u_m(t)$ should satisfy the PE (Persistently Exciting) property, and the input is generated in a consequent four-mode manner consisting of acceleration, positive constant velocity, deceleration, and negative constant velocity.

3.1 Two-mass motor system

Fig.3 show the motor drive system consisting of the two-mass motor with nonlinear frictions and the PI controller with unity gain which is employed to compensate stepwise torque disturbances. The motor and load are connected by a flexible shaft, and $u_p(t)$ is input torque, $\tau_c(t)$ torsional torque, $d(t)$ stepwise disturbance torque, $\omega_M(t)$ motor velocity, $\omega_L(t)$ load velocity. T_M[s] and T_L[s] are time constants of motor and load respectively, and T_C[s] is a shaft constant. The friction effects are also introduced such as viscous friction proportional to velocity and squared velocity and the Coulomb friction as illustrated in Fig.3, where D_M and D_L are motor damping constants of motor and load respectively, a and c denote nonlinear friction constants. The units are normalized by the maximum working velocity $\omega_{\max}$, hence T_M[s] implies the time in whcih the motor velocity changes from zero to $\omega_{\max}$ by the maximum working torque.

The purpose of the paper is to present an on-line identification algorithm for giving the above all physical model parameters $\{T_M,\ T_L,\ T_C,\ D_M.\ D_L,\ a,\ c\}$.

The state space representation of the above motor drive system is given by

$$\dot{\boldsymbol{x}}_p(t) = \boldsymbol{A}_p\boldsymbol{x}_p(t) + \boldsymbol{B}_p\xi(t) + \boldsymbol{A}_{\gamma p}\boldsymbol{\gamma}(\omega_M(t)) \tag{3a}$$

$$y_p(t) = \boldsymbol{C}_p(t)\boldsymbol{x}_p(t) \tag{3b}$$

where $\boldsymbol{x}_p = [\omega_M(t), \tau_C(t), \omega_L(t), x_{pi}(t)]^T$, and

$$\boldsymbol{A}_p = \begin{bmatrix} -\frac{D_M}{T_M} & -\frac{1}{T_M} & 0 & \frac{1}{T_M} \\ \frac{1}{T_c} & 0 & -\frac{1}{T_c} & 0 \\ 0 & \frac{1}{T_L} & -\frac{D_L}{T_L} & 0 \\ 0 & 0 & 0 & 0 \end{bmatrix},\ \boldsymbol{B}_p = \begin{bmatrix} \frac{1}{T_M} \\ 0 \\ 0 \\ \frac{1}{T_i} \end{bmatrix}$$

$$\boldsymbol{C}_p = [1 \quad 0 \quad 0 \quad 0]\ ,\ \boldsymbol{A}_{\gamma p} = \begin{bmatrix} -\frac{a}{T_M} & -\frac{c}{T_M} \\ 0 & 0 \\ 0 & 0 \\ 0 & 0 \end{bmatrix}$$

where the stepwise disturbance term is omitted in the above expression.

3.2 Construction of Reference Model

The major contribution of the paper is to clarify the role and structure of the reference model in order to de-

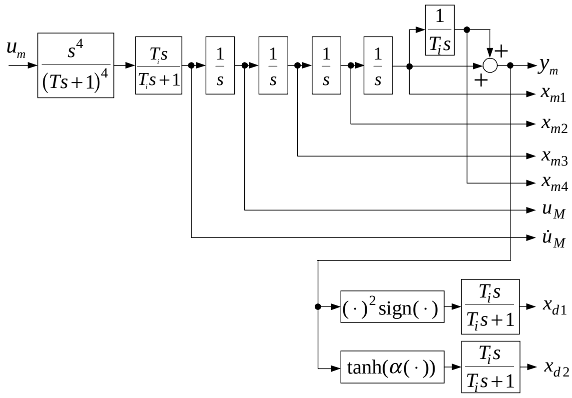

Figure 4: Reference model for two-mass motor

termine the physical model parameters in the closed-loop control. As shown in Fig.4, the role of the reference model is to generate the important signals which correspond to the actual signals in the two-mass motor system, as well as give the ordinary desired reference response. $u_m(t)$ is the reference input satisfying the PE property as mentioned before. The reference model consists of two roles: One is the reference input generation part for supplying the reference input $u_M(t)$, and the other is the reference model with the input $u_M(t)$ for adjusting the model parameters. The total desired reference input-output property from $u_m(t)$ to $y_m(t)$ is given by

$$y_m(t) = \frac{1}{(Ts+1)^4} u_m(t) \tag{4}$$

where T is a time constant of the total reference model.

The state space expression of the reference model with the input $u_M(t)$ is described by

$$\dot{\boldsymbol{x}}_m(t) = \boldsymbol{A}_m \boldsymbol{x}_m(t) + \boldsymbol{B}_m u_M(t) + \boldsymbol{A}_{\gamma m} \boldsymbol{\gamma}(y_m(t)) \tag{5a}$$
$$y_m(t) = \boldsymbol{C}_m \boldsymbol{x}_m(t) \tag{5b}$$

where $\boldsymbol{x}_m = [x_{m1}\ x_{m2}\ x_{m3}\ x_{m4}\ x_{m5}\ x_{m6}]^T$, and

$$\boldsymbol{A}_m = \begin{bmatrix} 0 & 1 & 0 & 0 & 0 & 0 \\ 0 & 0 & 1 & 0 & 0 & 0 \\ 0 & 0 & 0 & 0 & 0 & 0 \\ \frac{1}{T_i} & 0 & 0 & 0 & 0 & 0 \\ 0 & 0 & 0 & 0 & -\frac{1}{T_i} & 0 \\ 0 & 0 & 0 & 0 & 0 & -\frac{1}{T_i} \end{bmatrix}$$

$$\boldsymbol{B}_m = \begin{bmatrix} 0 \\ 0 \\ 1 \\ 0 \\ 0 \\ 0 \end{bmatrix}, \ \boldsymbol{A}_{\gamma m} = \begin{bmatrix} 0 & 0 \\ 0 & 0 \\ 0 & 0 \\ 0 & 0 \\ -\frac{1}{T_i} & 0 \\ 0 & -\frac{1}{T_i} \end{bmatrix}$$

$$\boldsymbol{C}_m = [1 \quad 0 \quad 0 \quad 1 \quad 0 \quad 0]$$

$$\boldsymbol{\gamma}(y_m(t)) = \begin{bmatrix} |y_m(t)|y_m(t) \\ tanh(\alpha \cdot y_m(t)) \end{bmatrix}$$

From Fig.2, the control input is given as

$$\xi(t) = \boldsymbol{K}^T(t)\boldsymbol{r}(t) \tag{6}$$

$$\boldsymbol{r}(t) = [e_y\ x_{m1}\ x_{m2}\ x_{m3}\ x_{m4}\ u_M\ \dot{u}_M\ x_{d1}\ x_{d2}]^T$$
$$\boldsymbol{K}(t) = [K_e\ K_{x1}\ K_{x2}\ K_{x3}\ K_{x4}\ K_{u_M}\ K_{\dot{u}_M}\ K_{d1}\ K_{d2}]^T$$

3.3 Identification of Physical Model Parameters

The adjustable parameters in (6) are updated as follows:

$$\dot{\boldsymbol{K}}(t) = e_y \boldsymbol{\Gamma} \boldsymbol{r}(t), \quad \boldsymbol{\Gamma} = \boldsymbol{\Gamma}^T \geq 0 \tag{7}$$

where $e_y(t) = y_m(t) - \omega_M(t)$.

By employing the controlled system (3) and the reference model (5) in the proposed scheme given in Fig.4, we can give the following convergence property of the adjustable parameter vector.

Property 1: Let the control law be given by (6) and the parameter adaptation law be given by (7) in the controlled system in the proposed structure in Fig.2. If the control input can force the output error $e_y(t)$ to zero, the adjusted parameters converge as

$$\begin{aligned} &\lim_{t\to\infty} K_{x1} = D_M + D_L \\ &\lim_{t\to\infty} K_{x2} = T_M + T_L - T_C D_L^2 \\ &\lim_{t\to\infty} K_{x3} = -2T_C T_L D_L + D_L^3 T_C^2 \\ &\lim_{t\to\infty} K_{x4} = 0 \\ &\lim_{t\to\infty} K_{u_M} = -T_C T_L^2 - T_C^3 D_L^4 + 3T_L T_C^2 D_L^2 \\ &\lim_{t\to\infty} K_{\dot{u}_M} = 3T_C^2 T_L^2 D_L - 4T_C^3 T_L D_L^3 - T_C^4 D_L^5 \\ &\lim_{t\to\infty} K_{d1} = a, \quad \lim_{t\to\infty} K_{d2} = c \end{aligned} \tag{8}$$

See Appendix 1. The property can be proved by the aid of the command generator tracker (CGT) theory which plays an important role in the simple adaptive control [6]. See Appendix 1 as for its proof. By neglecting higher orders of smaller parameters, we can solve (8) with respect to the physical parameters to be obtained, as

$$T_L \cong \frac{3K_{x3}K_{u_M}}{2K_{\dot{u}_M}}, \quad T_M \cong K_{x2} - T_L, \quad T_c \cong -\frac{4K_{\dot{u}_M}^2}{9K_{x3}^2 K_{u_M}}$$
$$D_L \cong \frac{3K_{x3}^2}{4K_{\dot{u}_M}}, \quad D_M \cong K_{x1} - D_L \tag{9}$$

Thus, the physical parameters can be calculated by (10) in an on-line way, and then the proportional gain $K_e(t)$ of the PI controller is tuned as $K_e(t) = \omega_C K_{x2}(t) = \omega_C(T_M + T_L)$.

Property 2: In the proposed control system in Fig.2, the output errors are bounded in a finite region specified by

$$\boldsymbol{D}(\boldsymbol{e}_x(t)) = \left\{ \boldsymbol{e}_x(t) \middle| \begin{array}{c} -\infty < e_{x1}(t) < \infty, \\ |e_{x2}(t)| + |e_{x3}(t)| + |e_{x4}(t)| < \frac{\beta}{\theta_1} \\ \frac{\theta_2}{\beta} < |e_{x2}(t)|, \frac{\theta_2}{\beta} < |e_{x3}(t)|, \frac{\theta_2}{\beta} < |e_{x4}(t)| \end{array} \right\}$$

4. Discrete-Time Implementation

Fig.5 illustrates digital implementation of the continuous-time algorithm proposed in the paper. The

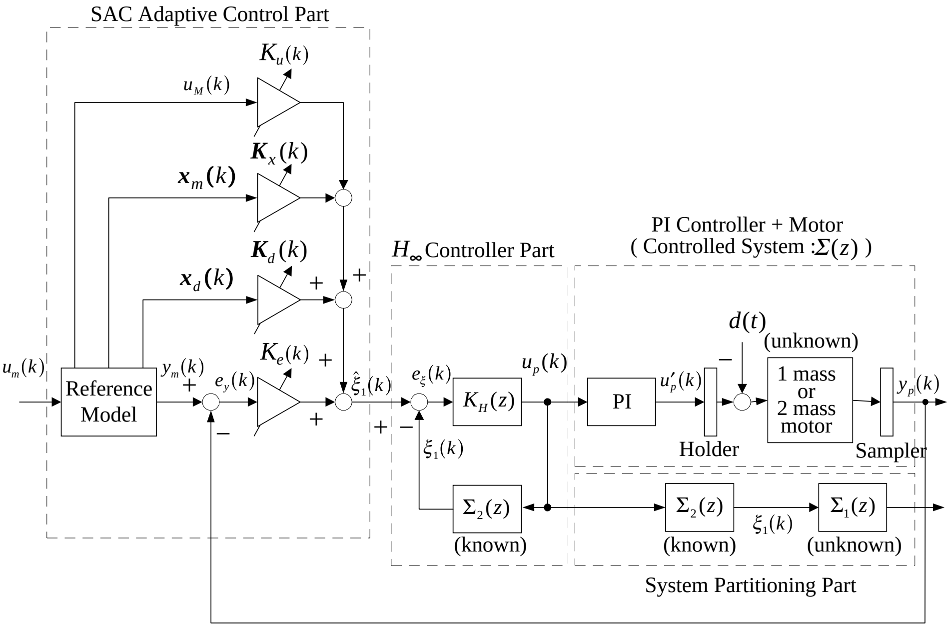

Figure 5: Digital implementation of the proposed closed-loop tuning

controlled system model discretized with a zero-order holder does not satisfy the ASPR property since the relative degree of the discrete-time model is one. Hence, a serial controller designed by H_∞ design theory is introduced to compensate the relative degree one [7]. In the simplified implementation, by replacing the designed transfer function from $\hat{\xi}_1(k)$ to $u_p'(k)$ by a phase-lead compensator, we design the compensator as:

$$u_p'(k) = [1 + (1 - z^{-1})]\hat{\xi}_1(k) \qquad (10)$$

where the frequency responsw of (10) is almost same as that of the compensator via H_∞ design in the working frequency range.

We take a δ-operation with lowpass filter to desctretize the proposed continuous-time adaptive algorithm, where $\delta = (z-1)/T$, T is a sampling interval. To reduce noise effects, a lowpass filter $1/E(\delta)$ is adopted to filter the signals involving noise, as $e_{yf}(k) = (1/E(\delta))e_y(k)$ and $\boldsymbol{r}_f(k) = (1/E(\delta))\boldsymbol{r}(k)$. Thus, the adaptive algorithm can be rewritten by using the flitered signals as

$$\begin{aligned}
&\hat{\xi}_1(k) = \boldsymbol{K}^T(k)\boldsymbol{r}_f(k) \qquad (11)\\
&\delta K_e(k) = e_{yf}(k)\gamma_e e_{yf}(k) - \sigma K_e(k)\\
&\delta K_{x1}(k) = e_{yf}(k)\gamma_{I1} x_{m1f}(k)\\
&\delta K_{x2}(k) = e_{yf}(k)\gamma_{I2} x_{m2f}(k)\\
&\delta K_{x3}(k) = e_{yf}(k)\gamma_{I3} x_{m3f}(k) - \rho_{x3}|e_{yf}(k)|K_{x3}(k)\\
&\delta K_{u_M}(k) = e_{yf}(k)\gamma_{I_{u_M}} u_{Mf}(k) - \rho_{u_M}|e_{yf}(k)|K_{u_M}(k)\\
&\delta K_{\dot{u}_M}(k) = e_{yf}(k)\gamma_{I\dot{u}_M} \dot{u}_{Mf}(k) - \rho_{\dot{u}_M}|e_{yf}(k)|K_{\dot{u}_M}(k)\\
&\delta K_{d1}(k) = e_{yf}(k)\gamma_{d1} x_{d1f}(k)\\
&\delta K_{d2}(k) = e_{yf}(k)\gamma_{d2} x_{d2f}(k)
\end{aligned}$$

where $\boldsymbol{r}_f(k) = [e_{yf}(k)\ \boldsymbol{x}_{mf}^T(k)\ u_{Mf}(k)\ \dot{u}_{Mf}(k)\ \boldsymbol{x}_{df}^T(k)]^T$, $\boldsymbol{K}(k) = [K_e(k)\ \boldsymbol{K}_x^T(k)\ K_{u_M}(k)\ K_{\dot{u}_M}(k)\ \boldsymbol{K}_d^T(k)]^T$, $\boldsymbol{x}_{mf}(k) = [x_{m1f}(k)\ x_{m2f}(k)\ x_{m3f}(k)\ x_{m4f}(k)]^T$, $\boldsymbol{x}_{df}(k) = [x_{d1f}(k)\ x_{d2f}(k)]^T$, $\boldsymbol{K}_x(k) = [K_{x1}(k)\ \ K_{x2}(k)\ \ K_{x3}(k)\ \ K_{x4}(k)]^T$, and $\boldsymbol{K}_d(k) = [K_{d1}(k)\ K_{d2}(k)]^T$.

We also apply the e_1-adaptation law [8] for updating the smaller parameters K_{x3}, K_{u_M} and $K_{\dot{u}_M}$. σ used in the σ modification [9] is chosen as $0 < \sigma \leq 1$ and

$$K_e(k) = \omega_c K_{x2}(k) \ \text{ if } \ K_e(k) \leq \omega_c K_{x2}(k) \qquad (12)$$

Thus, $K_e(k)$ converges to $\omega_c K_{x2}(k) = \omega_c(T_M + T_L)$ and then the PI controller is auto-tuned.

5. Simulation and Experimental Results

The effectiveness of the proposed scheme for adaptive identification and compensation for friction is investigated in experiments using an induction motor. The control purposes are the tracking ability to the reference velocity changes and the recovery performance to torque disturbances. We examined the effectiveness of the proposed algorithm in simulations and experiments of velocity control, where we used two induction motors connected by a flexible shaft, where one motor is a driving machine and the other is a load machine, and they constitute a two-mass system. By attaching a weight to driving motor or load motor, we can change an inertia ratio (load inertia/drive inertia) as 1/3, 1, 3, as shown in Fig.6. The motor velocity is measured by an incremental pulse encoder with resolution 1024[pulse/rev]. We validated the obtained identified physical parameters by comparison with the real parameter values which were obtained via off-line identification using the M-sequence method. The values are given as follows: $T_M = 0.23$[s],

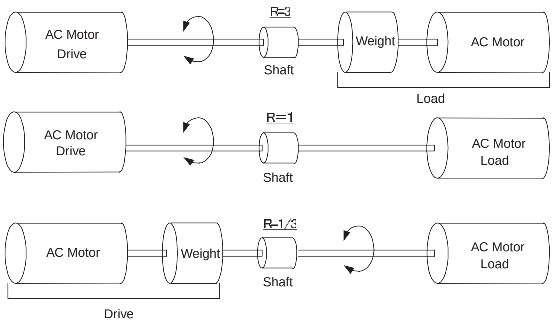

Figure 6: Two-mass system with changeable ineatia ratio

$T_C = 0.0016$[s], $D_M = D_L = 0.05$. Then, the experimental setup is given as follows: The sampling interval $T_s = 0.001$[s], the cut-off frequency is $\omega_c = 30$[rad/s], and then the integration constant is set at $T_i = 2/30$[s]. On the other hand, the time constant of reference model is chosen $T = 0.08$[s]. On the setup, we consider three cases with different inertia ratio R: (1) $R = 1 : (T_M = 0.23$[s], $T_L = 0.23$[s]), (2) $R = 3 : (T_M = 0.23$[s]), $T_L = 0.69$[s], (3) $R = 1/3 : T_M = 0.69$[s], $T_L = 0.23$[s].

Fig.7 shows simulation results of the adaptive identification and tuning algorithms. The reference output $y_m(k)$ is changed in various speed modes consisting of acceleration, constant velocity, decleration and zero velocity. 100% stepwise torque disturbances are added at 395 [s] in constant velocity and at 896 [s] in zero velocity. All the adjustable parameters are shown in Figs.7(b)(c). From these estimated parameters in the case $R = 1$, we can calculate the physical parameters from (9), which are plotted in Fig.7(d). Other physical parameters can also be identified similarly as in Figs.7(e)(f). All of the parameters converge their true values depicted by dotted lines, even in the presence of disturbances.

Fig.8 shows the experimental results in velocity control of an induction motor. As shown in Fig.8(a), the reference velocity is changed in four modes consisting acceleration, positive constant velocity, decleration, negative constant velocity, in which the unity velocity is normalized by the working velocity. By adding the weight to the motor or load machine, we can change the inertia ratios as $R = 1$, $R = 3$ and $R = 1/3$. The inertia and damping constants of motor and load, and shaft constant can be calculated from the adjustable parameters as stated before. The dotted lines indicate the physical parameters identified in an off-line identification using the M-sequence. In the initial interval until 150 [s], only larger parameters are updated and then all the parameters are updated after 150 [s]. It is seen from Figs, all the physical parameters converge to the constants which were obtained in off-line manners.8(b)$\sim$(d).

6. Conclusions

This paper has presented the new adaptive scheme for identifying the physical parameters of the motor drive

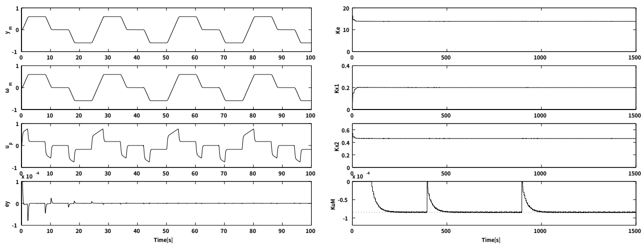

(a) y_m, ω_M, u_p and e_y (b) Adjustable parameters

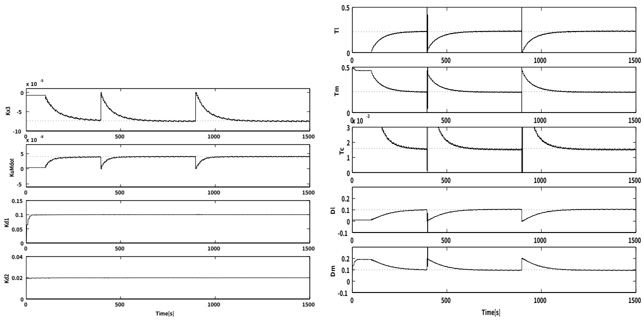

(c) Adjustable parameters ($R = 1$) (d) Physical parameters ($R = 1$)

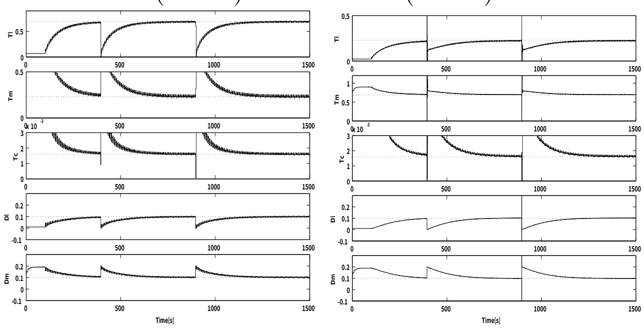

(e) Physical parameters ($R = 3$) (f) Physical parameters ($R = 1/3$)

Figure 7: Simulation results

system and compensating for friction effects in the feedforward manner. The proposed approach is characterized by the setup of the reference model which is derived from the physical structure of motor drive systems and generates the corresponding signals which are needed in the parameter adjustment. The convergence and stability have been investigated by assuming the ASPR property of the input-output relation of the controlled system. The serial compensation method has also been given to compensate for the non-ASPR property. Finally the experimental studies have validated the effectiveness of the proposed feedfoward type of the adaptive auto-tuning algorithm in velocity control of twp-mass induction motor.

References

[1] B. Armstrong-Helouvry, P. Dupont, and C. Canudas de Wit, "A survey of models, analysis and compensation method for the control of machines with friction", *Automatica*, vol. 30, no. 7, pp.1083-1138, 1994.

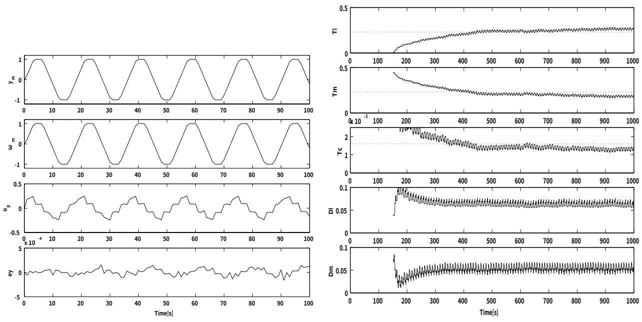

(a) y_m, ω_M, u_p and e_y (b) Inertia ration: $R = 1$

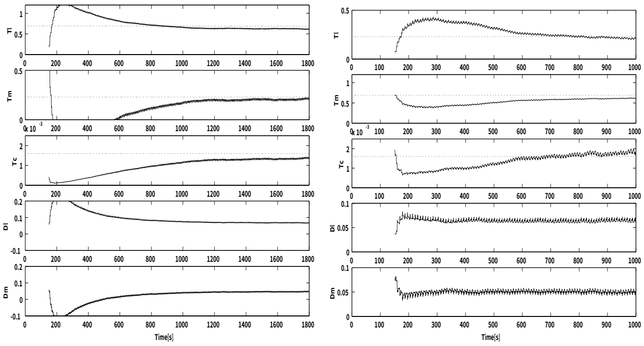

(c) Inertia ration: $R = 3$ (d) Inertia ration: $R = 1/3$

Figure 8: Experimental results

[2] K. Yuki, T. Murakami and K. Ohnishi, "Vibration control of a 2-mass resonant system by the resonance ratio control", Trans. IEE Japan, Vol.113-D, No.10, pp.1162-1169,1993.

[3] K. Sugiura and Y. Hori, "Vibration suppression in 2- and 3-mass system based on the feedback of imperfect derivative of the estimated torsional torque", IEEE Trans. Industrial Electronics, Vol.43, No.1, pp.56-64, 1996.

[4] S.N. Vukosavic and M.R.Stojic, "Suppression of torsional oscillations in a high-performance speed servo drive", IEEE Trans. Industrial Electronics, Vol.45, No.1, pp.108-117, 1998.

[5] K. Date, H. Ohmori, A. Sano, Y. Todaka and H. Nishida, "Speed control of two-mass resonant system by new simple adaptive control scheme", *Proc. the 7th IEEE Int. Conf. on Control Applications*, Trieste, Italy, pp.1120-1124, 1998.

[6] H. Kaufman, I. Bar-Kana and K. Sobel, *Direct Adaptive Control Algorithms*, Springer-Verlag, 1994.

[7] T. Dosho, H. Ohmori and A. Sano, "New design method of simple adaptive controll for system with arbitrary relative degree", *Proc. the 36th IEEE Conference on Decision and Control*, pp.1914-1917, 1997.

[8] K.S. Narendra and A. Annaswamy, "A new adaptive law for robust adaptation without persistently excitation" *IEEE Trans. Autom. Contr.,* Vol.AC-32, No.2, pp.134-145, 1987.

[9] P.A. Ioannou and Jing Sun, *Robust Adaptive Control*, Prentice Hall PTR, 1996.

Appendix: Proof of Properties 1 and 2

Proof of Property 1:

From the CGT theory, the ideal control input $\xi^*(t)$ can be given for the controlled system (3) and the reference model (5), as

$$\begin{aligned}&\boldsymbol{x}_p^*(t) = \boldsymbol{S}_{11}\boldsymbol{x}_m(t) + \boldsymbol{S}_{12}u_M(t) + \boldsymbol{S}_{13}\dot{u}_M(t)\\&\xi^*(t) = \boldsymbol{S}_{21}\boldsymbol{x}_m(t) + S_{22}u_M(t) + S_{23}\dot{u}_M(t) + \boldsymbol{S}_\gamma\boldsymbol{\gamma}(y_m(t))\end{aligned}$$

From (3), (5) and the above expression, it follows that $\dot{\boldsymbol{x}}_p^*(t)$ satisfies

$$\begin{aligned}\dot{\boldsymbol{x}}_p^*(t) &= \boldsymbol{S}_{11}\dot{\boldsymbol{x}}_m + \boldsymbol{S}_{12}\dot{u}_M(t)\\&= \boldsymbol{S}_{11}\boldsymbol{A}_m\boldsymbol{x}_m(t) + \boldsymbol{S}_{11}\boldsymbol{B}_m u_M(t)\\&\quad+\boldsymbol{S}_{11}\boldsymbol{A}_{\gamma m}\boldsymbol{\gamma}(y_m(t)) + \boldsymbol{S}_{12}\dot{u}_M(t)\\&= \boldsymbol{A}_p\boldsymbol{x}_p^*(t) + \boldsymbol{B}_p\xi^*(t) + \boldsymbol{A}_{\gamma p}\boldsymbol{\gamma}(y_m(t))\\&= [\boldsymbol{A}_p\boldsymbol{S}_{11} + \boldsymbol{B}_p\boldsymbol{S}_{21}]\boldsymbol{x}_m(t) + [\boldsymbol{A}_p\boldsymbol{S}_{12} + \boldsymbol{B}_pS_{22}]u_M(t)\\&\quad+[\boldsymbol{A}_p\boldsymbol{S}_{13} + \boldsymbol{B}_pS_{23}]\dot{u}_M(t) + [\boldsymbol{B}_p\boldsymbol{S}_\gamma + \boldsymbol{A}_{\gamma p}]\boldsymbol{\gamma}(y_m(t))\end{aligned} \tag{13}$$

Furhtermore, it leads from $y_m(t) \equiv \omega_M(t)$ that

$$\begin{aligned}y_m(t) &= \boldsymbol{C}_p\boldsymbol{x}_p^*(t)\\&= \boldsymbol{C}_p\boldsymbol{S}_{11}\boldsymbol{x}_m(t) + \boldsymbol{C}_p\boldsymbol{S}_{12}u_M(t) + \boldsymbol{C}_p\boldsymbol{S}_{13}\dot{u}_M(t)\\&= \boldsymbol{C}_m\boldsymbol{x}_m(t)\end{aligned} \tag{14}$$

Then we have from (13) and (14) that

$$\begin{aligned}&\boldsymbol{S}_{11}\boldsymbol{A}_m = \boldsymbol{A}_p\boldsymbol{S}_{11} + \boldsymbol{B}_p\boldsymbol{S}_{12},\quad \boldsymbol{S}_{11}\boldsymbol{B}_m = \boldsymbol{A}_p\boldsymbol{S}_{12} + \boldsymbol{B}_pS_{22}\\&\boldsymbol{S}_{12} = \boldsymbol{A}_p\boldsymbol{S}_{13} + \boldsymbol{B}_pS_{23},\quad \boldsymbol{S}_{11}\boldsymbol{A}_{\gamma m} = \boldsymbol{B}_p\boldsymbol{S}_\gamma + \boldsymbol{A}_{\gamma p}\\&\boldsymbol{C}_p\boldsymbol{S}_{11} = \boldsymbol{C}_m,\quad \boldsymbol{C}_p\boldsymbol{S}_{12} = 0,\quad \boldsymbol{C}_p\boldsymbol{S}_{13} = 0\end{aligned}$$

Then it follows that $\boldsymbol{S}_{21}$, S_{22}, S_{23}, $\boldsymbol{S}_\gamma$ are given by

$$\begin{aligned}\boldsymbol{S}_{21} &= [D_M + D_L \;\; T_M + T_L - D_L^2T_C\\&\quad -D_LT_C(-D_L^2T_C + 2T_L) \;\; 0 \;\; a \;\; c]\\S_{22} &= -T_CT_L^2 - T_C(D_L^4T_C^2 - 3D_L^2T_CT_L)\\S_{23} &= 3T_C^2T_L^2D_L,\quad \boldsymbol{S}_\gamma = [a \quad c]\end{aligned}$$

then the ideal control input $\xi^*(t)$ is

$$\begin{aligned}\xi^*(t) &= \boldsymbol{S}_{21}\boldsymbol{x}_m(t) + S_{22}u_M(t) + S_{23}\dot{u}_M(t) + \boldsymbol{S}_\gamma\boldsymbol{\gamma}(y_m(t))\\&= (D_M + D_L)x_{m1}(t) + (T_M + T_L - D_L^2T_C)x_{m2}(t)\\&\quad+(-D_LT_C(-D_L^2T_C + 2T_L))x_{m3}(t) + 0\cdot x_{m4}(t)\\&\quad+a\cdot x_{m5}(t) + c\cdot x_{m6}(t)\\&\quad+(-T_CT_L^2 - T_C(D_L^4T_C^2 - 3D_L^2T_CT_L))u_M(t)\\&\quad+(3T_C^2T_L^2D_L - 4T_C^3T_LD_L^3 - T_C^4D_L^5)\dot{u}_M(t)\\&\quad+a|y_m(t)|y_m(t)| + ctanh(\alpha\cdot y_m(t))\\&\cong (D_M + D_L)x_{m1}(t) + (T_M + T_L)x_{m2}(t)\\&\quad+(-2T_CT_LD_L)x_{m3}(t) + (-T_CT_L^2)u_M(t)\\&\quad+(3T_C^2T_L^2D_L)\dot{u}_M(t) + a\cdot x_{d1}(t) + c\cdot x_{d2}(t)\end{aligned}$$